Available online at www.sciencedirect.com
SCIENCE DIRECT
Biochimica et Biophysica Acta 1758 (2006) 468–478
BIOCHIMICA ET BIOPHYSICA ACTA
BBA
http://www.elsevier.com/locate/bba

Influence of the chain length of ubiquinones on their interaction with DPPC in mixed monolayers

Yann Roche [1], Pierre Peretti, Sophie Bernard *

Paris Descartes University, Biomedical research center, Laboratoire de Neuro-Physique Cellulaire, 45 rue des Saints-Pères, 75270 Paris Cedex 06, France

Received 14 October 2005; received in revised form 13 March 2006; accepted 14 March 2006
Available online 6 April 2006

Abstract

The thermodynamic behavior of representative short (UQ2), middle (UQ4 and UQ6) and long-chain (UQ10) ubiquinones (UQ) mixed with dipalmitoyl-phosphatidylcholine (DPPC) was studied in monolayers at the air–water interface. The influence of isoprenoid chain-length of UQ on miscibility of both lipids was investigated by analysis of surface pressure-area isotherms and using fluorescence microscopy. Analysis of excess areas (A_{ex}) and free energies of mixing (ΔG_m), calculated from compression isotherms in the full range of ubiquinones concentrations, has given evidences for UQ-rich constant-size (UQ6, UQ10) or less growth limited (UQ2, UQ4) microdomains formation within mixed films. Fluorescence microscopy observation revealed that ubiquinones are preferentially soluble in the expanded phase. When lateral pressure increased, concomitant evolutions of A_{ex} and ΔG_m parameters, and composition dependence of collapse surface pressures, argue for an evolution towards a total segregation, never reached due to expulsion of ubiquinones from the film. The possible significance of these observations is discussed in relation to ubiquinones organization and similar chain length effects in membranes.

Keywords: Mixed monolayer; Ubiquinone; Fluorescence microscopy; Molecular interaction; Miscibility

1. Introduction

Ubiquinones are known to act as mobile lipophilic redox components of transmembrane electrons transport systems of eukaryotic and prokaryotic organisms. These compounds, also named coenzymes Q, consist of a redox-active 2,3-dimethoxy-5-methylbenzoquinone ring with a hydrophobic isoprenoid side chain in the 6 position. Ubiquinones (UQn) differ from one to another in the length of their side chain as indicated by a number (n) following the name, which is ranging between 2 and 10 isoprene units (2-methyl-2-butene) [1,2]. Thus ubiquinone 10 (UQ10) indicates a quinone with a side chain containing 10 isoprene units or 50 carbon atoms. They have been isolated for the first time in 1957 from bovine heart mitochondria by F.L. Crane and have been described the same year by Crane et al. [3], Morton et al. [4], Ernster and Dallner [5].

Ubiquinone 10 is the major physiological form of ubiquinones found in animals and humans. Its main function is to act as a coenzyme in the respiratory chain of the inner mitochondrial membranes by laterally transferring electrons from the complex I (or complex II) to complex III and transporting protons across the membrane by transverse diffusion, as described by P. Mitchell in 1976 when he introduced his famous "Q cycle" [6,7]. Now, it is well established that, in addition to these bioenergetic functions, ubiquinones, in their reduced form (ubiquinols), serve also as lipid-soluble antioxidants. Indeed, as suggested in 1961 by Kaufmann and Garloff [5,8], an antioxidant function of UQ was found to protect against lipid peroxidation in the membrane, to prevent DNA damage and serum low-density lipoproteins peroxidation [5]. Moreover, ubiquinones can regenerate vitamin E [9], another powerful antioxidant. Ubiquinones could also have a prooxidant action [10] since the reaction of the semi-quinone radical with O_2 produces a superoxide radical. Lastly, roles in the control of cell growth [11–13] and apoptosis [14,15]

* Corresponding author. Tel.: +33 1 42 86 20 46; fax: +33 1 42 86 20 85.
E-mail address: Sophie.Bernard@univ-paris5.fr (S. Bernard).
[1] Present address: Unité MéDIAN, UMR CNRS 6142, Faculté de Pharmacie de Reims, 51 rue Cognacq-Jay, 51096 Reims cedex, France.

0005-2736/$ - see front matter © 2006 Elsevier B.V. All rights reserved.
doi:10.1016/j.bbamem.2006.03.015

have also been reported recently. Indeed, ubiquinones seem able to regulate inhibition or activation of apoptosis by their pro- and antioxidant properties or by direct interactions with systems known to control this cell-death process.

The ever-increasing use of ubiquinones for the treatment of a great variety of pathologies, including myopathies, [16–20] cardiovascular diseases [21–23] and age related degenerative diseases, [24–26] has considerably stimulated medical interest in these natural molecules. Although UQ10 is the human homologue, some clinical studies showed that the short-chain analogues have a greater medical efficiency than exogenous UQ10 [27]. Moreover, several studies have pointed out that complex I of the mitochondrial respiratory chain has two distinct anchoring sites for short-chain and long-chain ubiquinones [28–30]. This result suggests that the biological action of ubiquinones could depend on their lateral chain length.

Hence, studying the localization and the molecular organization of ubiquinones in membrane is essential for understanding how their roles in biological membranes, and then their medical efficiency, could depend on their chain length. Indeed, the role of the polyisoprene domain in UQ mobility, redox reactions, location within the membrane is not unequivocally explained. In a previous paper [31], we used mixed monomolecular films containing phospholipids and UQ2 or UQ10. Our conclusions had pointed out that UQ2 would have their benzoquinone rings located nearer the headgroup of phospholipids, their side chain parallel to phospholipids acyl chain, while UQ10 would rather lie parallel to the membrane plane in the bilayer center, as stated by some authors using bilayers as model membranes. Indeed, ^{1}H-NMR study [32] and NMR measurements of ^{13}C-labeled ubiquinones [33] have both shown that short-chain ubiquinones (UQ2, UQ3) are located near the bilayer surface, while UQ10 seems entirely located near the bilayer midplane. Several differential scanning calorimetry (DSC) studies have allowed drawing the same conclusions by following ubiquinones influence on phospholipids vesicles thermodynamic parameters ([34–36] and Roche, Y. et al., unpublished data). In contrast, other workers using fluorescence anisotropy techniques have suggested that the UQ10 benzoquinone ring interacts with the phospholipids polar heads, while their side chain would remain anchored to the hydrophobic bilayer midplane [37]. Based on linear dichroism and fluorescence quenching experiments, Lenaz et al. [38], Samori et al. [39] have studied the orientation of ubiquinones in bilayers and concluded that, even if they tend to oscillate between the two bilayer surfaces, long-chain ubiquinones may spend statistically longer times at the midplane. More recently, Hauss et al. [40] have shown that the polyisoprene domain of UQ10, like that of squalane, [41] lies in the center of the hydrophobic core parallel to the membrane plane and not parallel to the lipid chains. Thus, quinone polyisoprenoids may inhibit proton leakage in addition to their other biological roles.

The present study aims to provide new insights about the influence of chain-length on the organization of ubiquinones in monolayers. We report here a systematic and comparative study of four ubiquinones and their mixing with dipalmitoyl-phosphatidylcholine (DPPC) at the air–water interface, using the film balance technique. UQ with two (UQ2), four (UQ4), six (UQ6) and ten isoprene units (UQ10) have been used as representative of short to long-chain quinones. Information about miscibility of the components and thermodynamical data were deduced from analysis of surface pressure-area isotherms. Observation of mixed monolayers by epifluorescence microscopy has permitted us to study the changing sizes and shapes of condensed domains as a function of the molar fraction of ubiquinone.

2. Materials and methods

2.1. Materials

Ubiquinone 2 (UQ2), ubiquinone 6 (UQ6) and ubiquinone 10 (UQ10) were purchased from Sigma Aldrich (France), whereas ubiquinone 4 (UQ4) was supplied by Fluka (France). All the ubiquinones were used without further purification. L-α-dipalmitoyl phosphatidylcholine (DPPC) was of the purest available quality from Sigma. The fluorescent probe, 2-(6-(7-nitrobenz-2-oxa-1, 3-diazol-4-yl)amino)hexanoyl-1-hexadecanoyl-*sn*-glycero-3-phosphocholine (NBD-PC) was obtained from Molecular Probes Inc. (USA). Chloroform was of analytical grade from Fisher Scientific Co. (France). The subphase was pure water treated on an Elgastat UHQ 2 system (resistivity of 18 MΩcm). Stock solutions of the four ubiquinones and DPPC, 10^{-3} M or 2.5×10^{-4} M, were prepared in chloroform, or chloroform/methanol 90:10 (v:v) for UQ10, and spread separately or mixed in the wanted molar ratios.

2.2. Surface-pressure isotherms

Isotherms were performed with a Nima model 611M trough (Nima Technologies, England). The surface pressure was measured by the Wilhelmy plate method. The films were spread with Hamilton 1705 RN or 1710 RN microsyringes. The film compression started at least 20 min after spreading the lipids to allow solvent evaporation and was achieved at a speed of 4.5 Å^2/min/molecule. All experiments were performed at pH 5.7 and at a temperature of 22 °C. All surface pressure-area isotherms presented here are the average of three to five experiments. Data analysis was done with Origin 5.0 from Microcal Software.

2.3. Epifluorescence microscopy

Visualization of monolayers was done by means of an Olympus-BX30 microscope, set on a Riegler and Kirsten Langmuir trough. Excitation of the probe is achieved using high-pressure mercury lamp. Discrimination of excitation (470 nm) and emission (530 nm) fluorescence from the dye (NBD-PC) is regulated by dichroic mirrors and interchangeable cut-off filters. An AIS (MXRi2) video camera with an image intensifier which allows a very high sensitivity (10^{-6} Lux) enables us to visualize the monolayer and to record images. These experiments were also performed at a temperature of 22 °C and at pH 5.7. Mixtures were prepared from a chloroform solution of DPPC containing the wanted proportions of ubiquinone and 0.5 mol% NBD-PC. The probe is excluded from densely packed areas of lipid, providing contrast between lipid phases. Images were recorded during the continuous low speed (0.2 Å^2/min/molecule) symmetric compression of the monolayer and their features were analyzed using digital image analysis software OPTIMAS 5.1 (Optimas Corporation). The percentage of dark region was estimated by division of the total amount of probe-excluded regions by the total area of a frame. Our homemade acquisition software allows surface pressure to be measured simultaneously with image grabbing. The accuracy of surface pressure measurements is ±0.5 mN/m.

3. Results

3.1. Pure UQn monolayers

The surface pressure-area isotherms for pure ubiquinones with different side-chain length performed at 22 °C on a water

subphase are shown in Fig. 1. All the studied UQ were capable of forming monolayers at the air/water interface. The curves do not show the presence of the transition from liquid-expanded to liquid condensed state as observed in pure DPPC monolayers. As the number of isoprene units in the molecules increases, the surface pressure-area curves shift, at a given surface pressure below the collapse, to greater values of area per molecule. For surface pressure up to 3 mN/m, isotherms of UQ6 and UQ10 overlap. UQ6 occupies a greater molecular area than UQ4 below 12 mN/m.

The limiting areas per molecules, obtained by extrapolation of the linear parts on the isotherms to the abscissa, of UQ2, UQ4, UQ6 and UQ10 are 48.05, 59.35, 65.94 and 70.82 Å^2, respectively. The limiting areas increase with the side chain length. The addition of two isoprene units clearly causes more pronounced changes in the area for short homologues than for the long ones.

The compressibility κ was calculated at 5 and 10 mN/m according to Eq. (1) (where A is the molecular area in the film at a fixed surface pressure) and plotted in Fig. 2A as a function of the number of isoprene units.

$$\kappa = -\frac{1}{A}\left(\frac{\partial A}{\partial \pi}\right)_T. \quad (1)$$

At 5 mN/m, compressibilities of UQ2, UQ4 and UQ10 are close to that of DPPC (about 32 m/N), while such a κ value reaches at 10 mN/m for UQ6. At this surface pressure, the variation of κ of UQ2, UQ4 and UQ6 seems to be more sensitive to the chain length, even if κ of UQ10 is close to that of UQ6.

The collapse pressures π_c of the monolayer, corresponding to the surface pressures at the transition point from monolayer to three-dimensional multilayer films, were determined from the inflection points on the curves and are presented in Fig. 2B as a function of the number of isoprene units. Among the four ubiquinones investigated, the most hydrophobic one, UQ10 (ten isoprene units, i.e., 50 carbon atoms) has formed monolayers with the lowest collapse pressure. UQ2 shows the highest collapse pressure as the most polar molecule of the series. As the length of the side-chain decreases, the monolayers become more stable to higher pressures. Our data exhibit an exponential decrease of π_c with the number of isoprene units.

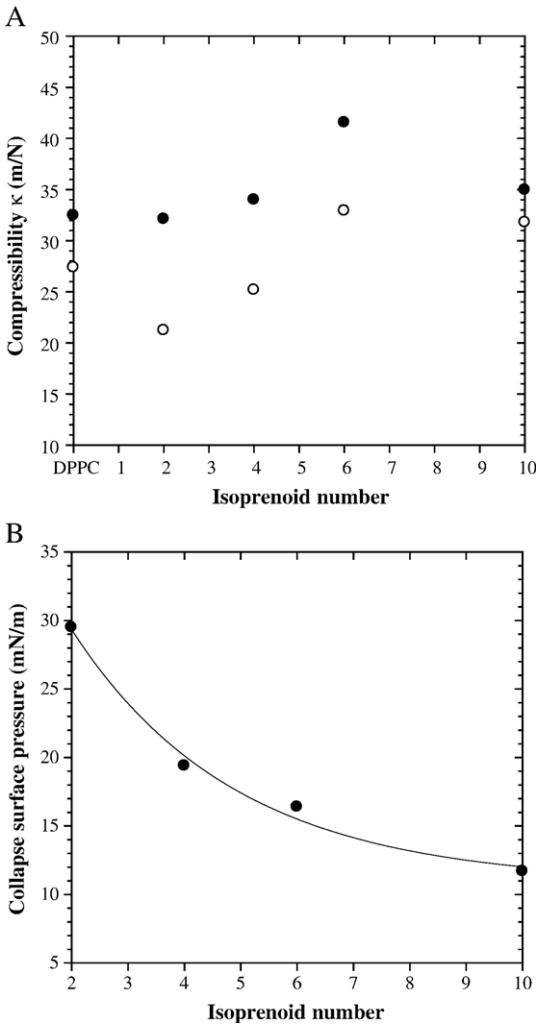

Fig. 2. (A) Variation of the compressibility as a function of the number of isoprene units. Values of κ were determined at 5 mNm^{-1} (●) and at 10 mNm^{-1} (○) from isotherms of pure UQ monolayers. (B) Collapse surface pressures of pure UQ monolayers as a function of the number of isoprene units, determined from the inflection points on the compression isotherms.

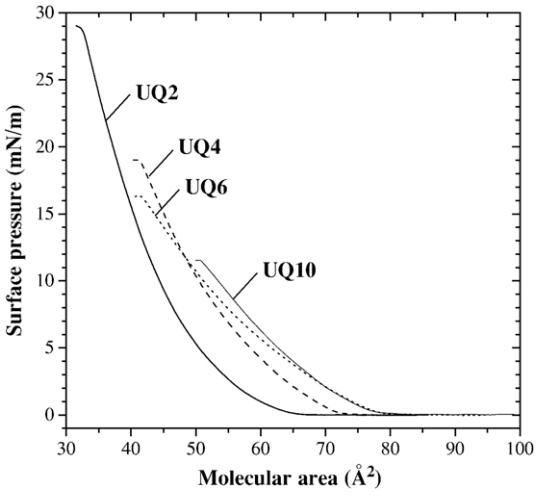

Fig. 1. Compression isotherms of pure UQ monolayers spread on water subphase (pH 5.7) at 22 °C.

For each UQ, the pure film could be compressed to very low areas (below 20 Å^2) without observing a decrease in pressure (data not shown). This is not consistent with the van der Waals dimension of a methyl-branched hydrocarbon chain oriented in close-packed array which is about 45 Å^2 [42]. This observation suggests that a loss of material occurs during the compression: ubiquinones could be progressively squeezed out of the film.

In order to evaluate the proportion of the material that was squeezed out from the monolayer at a given surface pressure, we have investigated the hysteresis of isotherms of pure UQ monolayers during compression-expansion cycles. In the first cycle of compression and expansion of the monolayer, negative hysteresis (i.e., decrease in area at a given pressure between the compression and the expansion segments of an isocyle) were

Table 1
Percentages of loss of UQ in monolayers at different surface pressure below the collapse (π_c) calculated from two compression-expansion cycles

Compound	At $\pi_c/4$	At $\pi_c/2$	At π_c	π_c (mN/m)
UQ2	2%	5%	9.2%	29.5
UQ4	1%	3.2%	7%	19.4
UQ6	1%	3%	5.4%	16.4
UQ10	1%	2%	8.5%	11.7

always observed for all the studied UQ (data not shown). This type of hysteresis is mostly observed [43] and could usually be attributed to: (i) incomplete dissolution of the sample into the spreading solvent, (ii) loss of molecules due to partial dissolution into the subphase, (iii) film collapse or multilayer formation during compression of the amphiphilic molecules. No precipitates were detected in the UQ solutions. When we spread different concentrations of UQ solutions, the surface pressure-area isotherms were identical. Therefore, explanation (i) is excluded. To evaluate the percentage of loss of material, we have examined two consecutive isocycles from the same monolayer, at three different target pressures: $\pi_c/4$, $\pi_c/2$ and π_c. In all cases, a strong dependence of the target pressure (π_t) on the hysteresis was observed. More π_t was close to π_c, more the hysteresis was enhanced. The influence of the chain length on the hysteresis was also observed. For the calculation of the mean percent content, we used the following formula:

$$\%loss = \frac{\Delta A}{A} \times 100 \quad (2)$$

where ΔA is the decrease in area between the first and the second compression isotherms and A is the area per molecule obtained during the first compression at a given surface pressure. As ΔA varies with the pressure, we used a mean value of ΔA during all the compression between 0 mN/m and π_t. Table 1 lists the percentages of loss of UQ in the monolayer. The percentage of loss is found to increase with π_t value. In addition, as the chain length increases, the percentages of loss of UQ are found to decrease except for UQ10 when the isocycles are performed up to the collapse pressure.

3.2. Mixed DPPC:UQn monolayers

Compression isotherms of DPPC–UQn mixtures, performed on pure water subphase (pH 5.7) for the following mole fraction of UQ: 0.01, 0.05, 0.1, 0.25, 0.5, 0.75, are shown in Fig. 3 as a function of the area per DPPC molecule in the film (i.e., without accounting UQ area contribution). The characteristic plateau of the first order transition between liquid expanded LE and liquid condensed LC states in the isotherm of pure DPPC at a pressure of about 7 mNm^{-1} was found to vanish with increasing ubi-

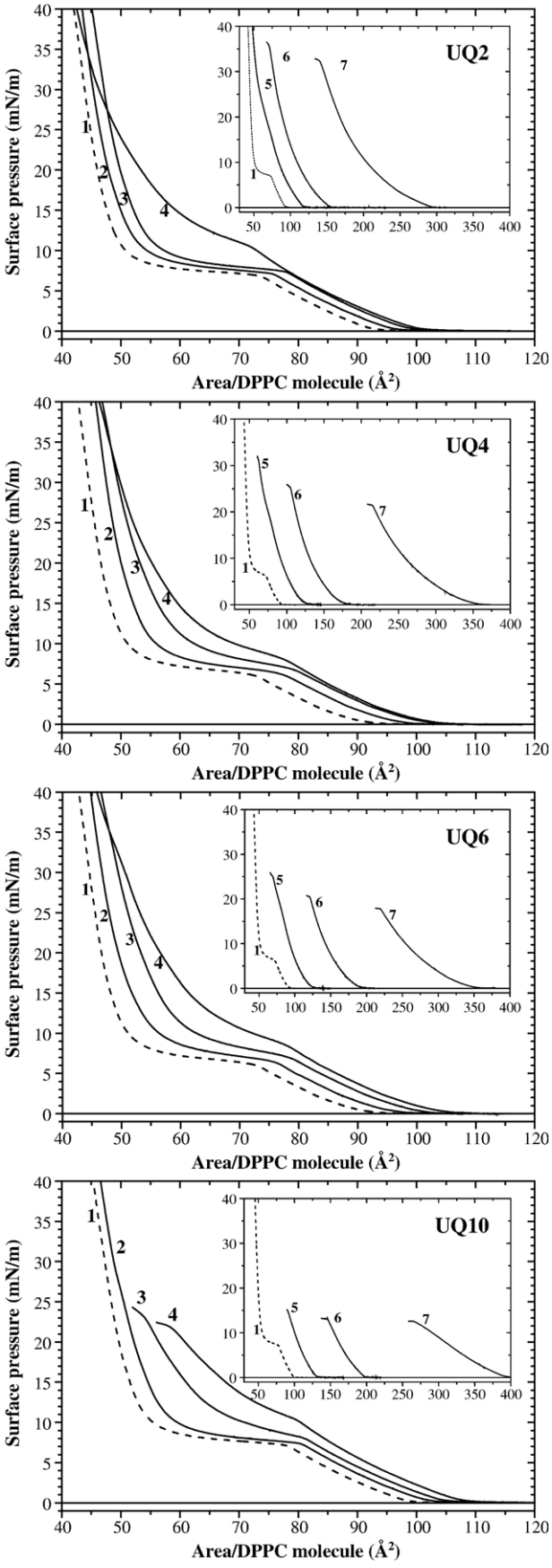

Fig. 3. Compression isotherms of mixed DPPC–UQn monolayers spread on water subphase (pH 5.7) at 22 °C. Surface pressure expressed as a function of the area per DPPC molecule for mixtures containing from 1 mol% to 75 mol% UQ2, UQ4, UQ6 and UQ10. Curve (1) corresponds to the pure DPPC isotherm (dashed line) and mixtures composition is: 1 mol% (2), 5 mol% (3), 10 mol% (4), 25 mol% (5), 50 mol% (6) and 75 mol% (7).

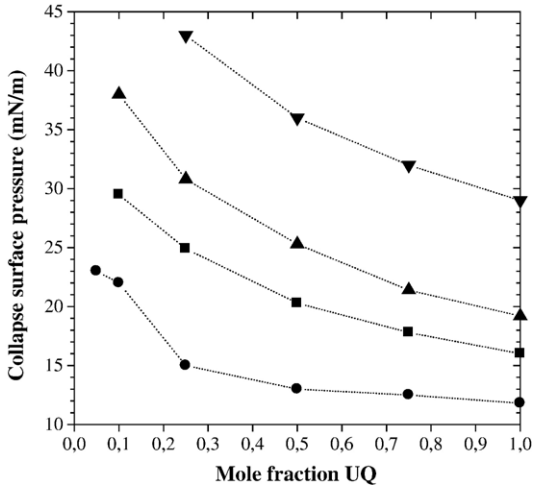

Fig. 4. Collapse surface pressures of mixed DPPC–UQ monolayers as a function of the ubiquinone mole fraction: UQ2 (▼); UQ4 (▲); UQ6 (■); UQ10 (●).

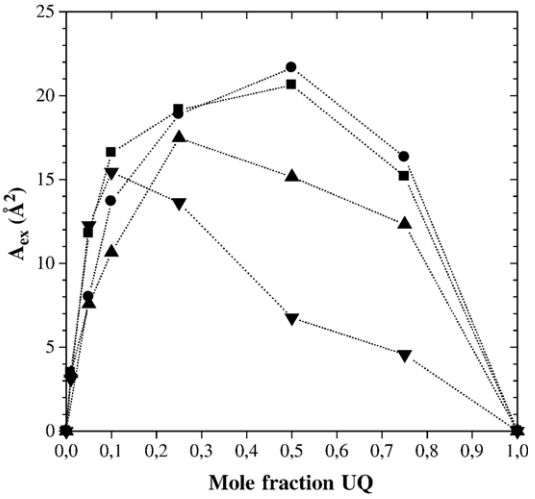

Fig. 5. Excess area of the mixed DPPC–UQ monolayers as a function of the ubiquinone mole fraction: UQ2 (▼); UQ4 (▲); UQ6 (■); UQ10 (●) at a surface pressure of 10 mNm^{-1}. Dot lines between the experimental points are simply a visual guide.

quinone content in the mixture. At 25%mol ubiquinones (Fig. 3, trace 5), the plateau has completely disappeared in all cases.

According to the phase rule, if the two components in the mixed monolayers are miscible, the collapse surface pressure should vary with composition [44,45]. It is obviously shown in Fig. 4 that the collapse surface pressures of mixed DPPC-UQn monolayers varied with composition. The data show a decrease with the UQ concentration, more pronounced in the case of UQ2, UQ4 and UQ6 than that observed for UQ10. In this last case, there are no significant variations of the collapse surface pressure above 50 mol% UQ10 in the film.

A quantitative analysis of the interaction between DPPC and UQ is provided by comparing, at a given surface pressure, the experimental average area per molecule of a mixed monolayer with that calculated assuming ideality of the mixing through the additivity rule [46,47] to give the excess area of mixing,

$$A_{ex.} = A_{12} - (X_1 A_1 + X_2 A_2) \quad (3)$$

where A_{12} is the mean molecular area at a given surface pressure in the two-component film, X_1 and X_2 the mole fractions of the components in the mixed monolayer, and A_1 and A_2 the molecular areas in pure monolayers of components 1 and 2 at the same surface pressure. The excess area, A_{ex}, can also be an indication of miscibility. Indeed, if an ideal mixed monolayer is formed or the two components are completely immiscible, the excess area will be zero and a plot of A_{12} will be linear in X_1 at a given surface pressure. Any deviation would indicate miscibility and non-ideality. Fig. 5 illustrates the excess area per molecule for the DPPC–UQ mixtures studied as a function of the mole fraction of ubiquinone. The additivity rule enables us to examine interactions of components in a mixed monolayer only below the collapse pressure of the component with the lowest π_c. Because of loss of material at higher pressure than about 13 mNm^{-1} in the case of UQ10 mixtures, the surface pressure value of 10 mNm^{-1} was chosen in order to compare the behavior of all the quinones. Moreover, the molecular area expansion was the most important at surface pressures around this value, and the loss of UQ was rather weak. Fig. 5 shows that positive deviations from ideality are observed for all the quinones and all compositions at 10 mNm^{-1}. These positive deviations from ideality indicate an expansion of monolayers and give strong evidence for repulsive interactions between ubiquinones and DPPC. Since a linear relationship between molecular area and composition is not observed, DPPC and UQ_n are considered to be miscible and form non-ideal monolayers at the interface [46]. The maximum deviation of the experimental data from the theoretical ones for an ideal mixture is observed at 50 mol% for both UQ6 and UQ10 mixtures. Theses results suggest that the incorporation of UQ6 or UQ10 into a DPPC monolayer may increase interactions between molecules in the mixed monolayers and the influence of intermolecular interaction on molecular packing is significant. The $A_{ex}=f(X_{UQ})$ profile is symmetric, i.e., excess area is proportional to the number of associations between DPPC and UQn molecules. The relative organization of both components, the one compared to the other in the mixed film, seems to be

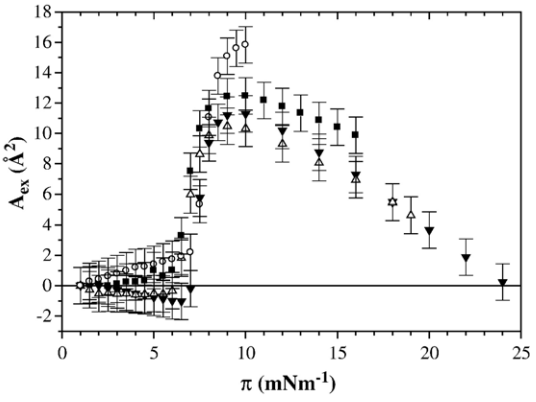

Fig. 6. Differential deviations from ideality ΔA_{ex} as a function of surface pressure for mixed DPPC–UQ monolayers containing 25 mol%: UQ2 (▼); UQ4 (△); UQ6 (■); UQ10 (○).

unchanged whatever the proportion. In the case of UQ4 and UQ2, the $A_{ex}=f(X_{UQ})$ profile is asymmetric, deviations from ideality being maximum at 25 mol% and 10 mol%, respectively. This suggests that above these contents DPPC:UQn interactions in mixed films would be minimized due to a change in the relative organization of both components.

We also introduced the differential deviation from ideality $\Delta A_{ex}=A_{ex}(\pi)-A_{ex}(\pi\rightarrow 0)$, where $A_{ex}(\pi)$ and $A_{ex}(\pi\rightarrow 0)$ are the excess area per molecule for DPPC:UQ mixtures, respectively, at a given surface pressure and at π close to zero, monolayers being assumed in a two-dimensions gaseous state. Variations of ΔA_{ex} with surface pressure for 25 mol% DPPC:UQ mixtures are depicted (Fig. 6). In all cases, deviation from ideality did not significantly vary between 1 and 6 mNm^{-1} and strongly reached to a maximum within 6–9 mNm^{-1} range. Interestingly, this interval corresponds to the LE/LC transition for pure DPPC. This suggests that miscibility of DPPC and UQn would be strongly modulated by the physical state of the monolayer, i.e., condensed or expanded.

Deviations from ideality can also be expressed in term of free energies of mixing, as in the treatment of mixing in the bulk state. The values of excess free energy ΔG_{ex} were calculated from the difference between areas under the isotherms of mixed and pure films for a specified surface pressure, following the mathematical method of Simpson and according to the Goodrich approach [48]:

$$\Delta G_{ex}(\pi)=\int_{\pi\rightarrow 0}^{\pi}(A_{12}-X_1A_1-X_2A_2)d\pi \quad (4)$$

Then, the total free energies of mixing were calculated according to the following relation:

$$\Delta G_m(\pi)=\Delta G_{ex}+RT(X_1\ln X_1+X_2\ln X_2) \quad (5)$$

where R is the gas constant and T is the temperature, and $\Delta G_{ideal}=RT(X_1\ln X_1+X_2\ln X_2)$ is the ideal free energy of mixing.

The total free energies of mixing ($\Delta G_{ex}+\Delta G_{ideal}$) were calculated at different surface pressures. The plot of ΔG_m versus the mole fraction of ubiquinone at various surface pressures is displayed in Fig. 7 with the ideal free energies of mixing for comparison. The excess free energies ΔG_{ex} are positive, i.e., $\Delta G_m>\Delta G_{ideal}$, at all the studied surface pressures and depend on the monolayer composition.

The positive ΔG_{ex} confirms repulsive interactions between DPPC and UQn and implies that these interactions are energetically unfavorable. Globally, at given surface pressure and composition, ΔG_m increases with the UQn chain-length, except for DPPC–UQ10 mixtures, where ΔG_m values are close to those of DPPC–UQ6. In addition, shapes of the $\Delta G_m=f(X_{UQ})$ profiles are analogous for each kind of mixtures, except for DPPC–UQ2 mixtures, where ΔG_m decreases for molar fractions higher than 25%mol, as previously observed for $A_{ex}=f(X_{UQ})$. Moreover, our results show that the ΔG_m values become positively larger as the surface pressure increases, suggesting that DPPC–UQn interactions are stronger and the mixed monolayers become less stable at higher surface pressures.

3.3. Epifluorescence microscopy of DPPC–UQn monolayers

DPPC:UQ_n mixtures containing weak ubiquinones molar fractions (1, 5 and 10 mol%) were observed by epifluorescence microscopy at the air–water interface. Fig. 8 shows a set of

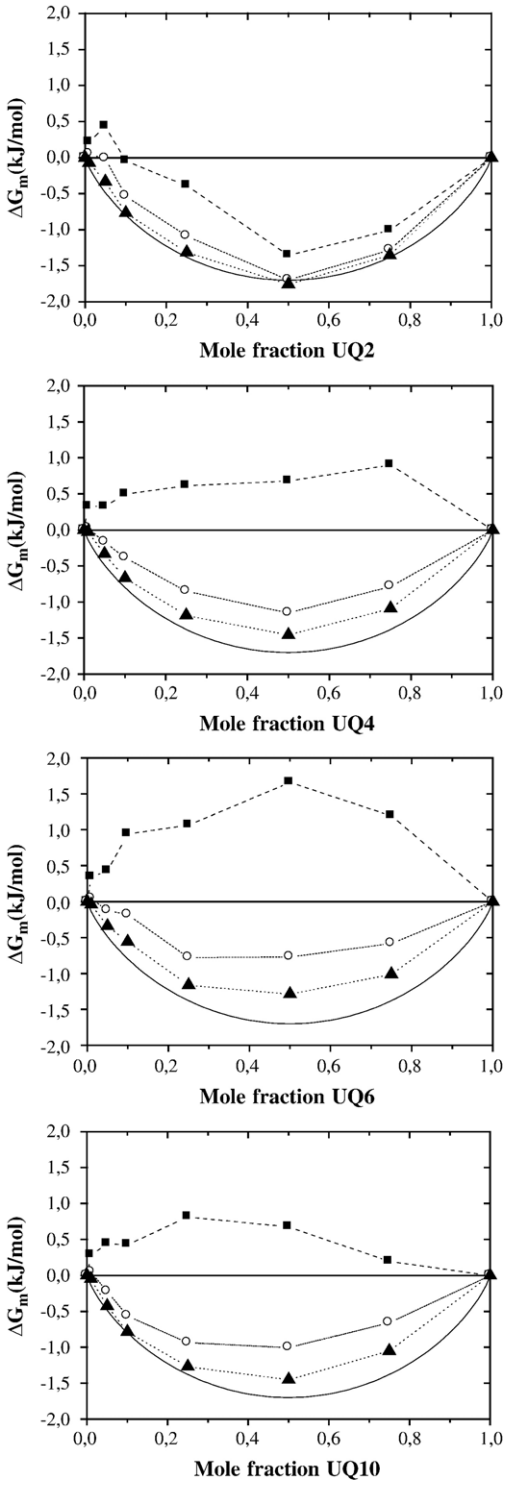

Fig. 7. Total Gibbs free energies of mixing ΔG_m as a function of composition for mixed DPPC–UQ monolayers at various surface pressures: (▲) 5 mN/m, (○) 10 mN/m, (■) 25 mN/m, compared with the ideal free energy of mixing ΔG_{ideal} (solid line).

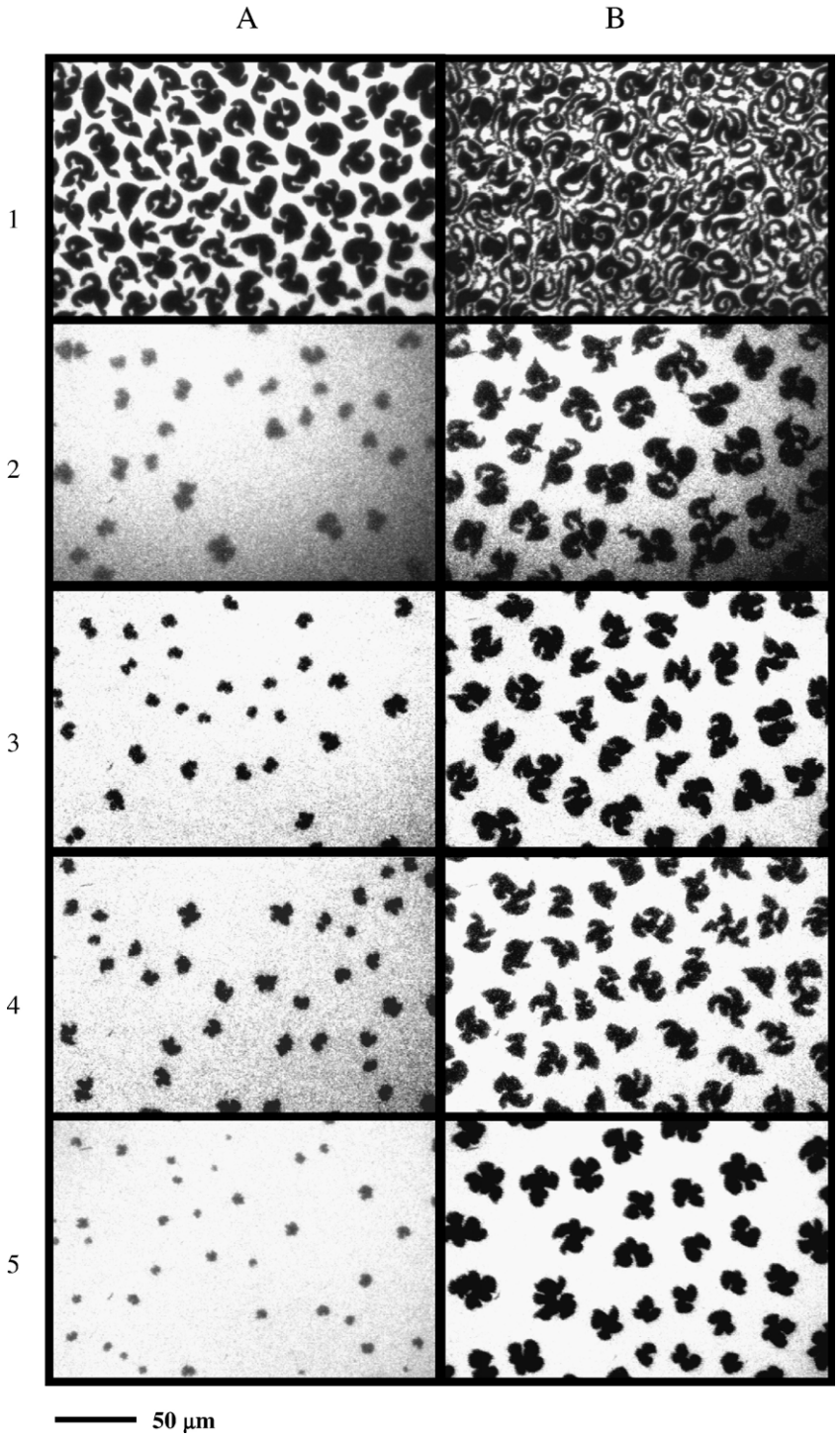

Fig. 8. Fluorescence microscopy images of monolayers at 6 mN/m (A) and 8 mN/m (B). (1) DPPC:NBD-PC (99.5:0.5), (2) DPPC:NBD-PC:UQ2 (94.5:0.5:5), (3) DPPC:NBDPC: UQ4 (94.5:0.5:5), (4) DPPC:NBD-PC:UQ6 (94.5:0.5:5), (5) DPPC:NBD-PC:UQ10 (94.5:0.5:5).

images obtained when monolayers of DPPC:NBD–PC:UQ 94.5:0.5:5 on pure water were compressed at the same rate without interruption for video recording.

At surface pressures near to zero, images observed for all the monolayers consist of dark circular "bubbles" of 2D gas in the bright field of the liquid-expanded (LE) phase (data not shown). At low pressures (1–5 mNm^{-1}), pure DPPC monolayers showed the homogeneous fluorescent LE phase due to a result of dye partitioning. In mixed DPPC:UQ monolayers, the bright field of the less ordered LE phase persists at higher surface pressures as the mole fraction of ubiquinone increased. Then, as surface pressure is increased further in monolayers, transition into liquid-condensed phase occurs, indicated by the appearance of dark LC domains. Indeed, the condensed phase is dark since the dye is excluded from the ordered domains due to steric hindrance. These domains were relatively homogenous in shape

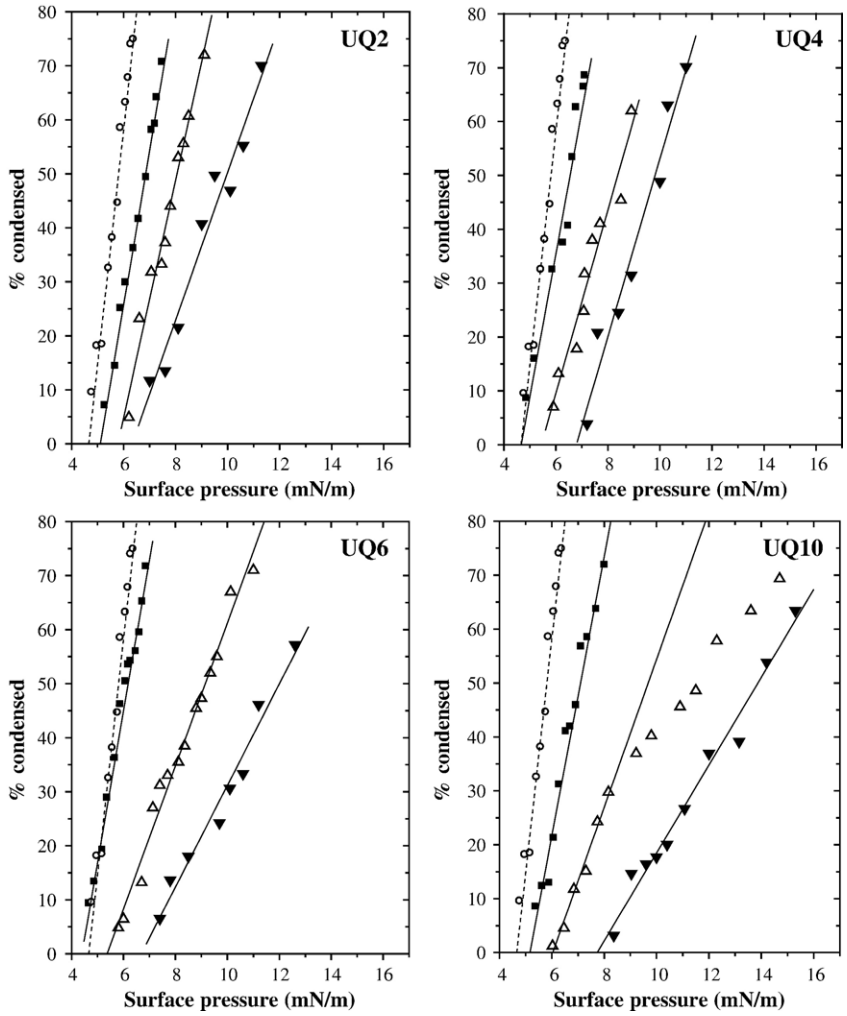

Fig. 9. Fluorescence microscopy of monolayers: total percentage of dark (probe excluded) regions per frame, plotted as a function of surface pressure for: (○) pure DPPC, (■) 1 mol% UQ, (△) 5 mol% UQ, (▼) 10 mol% UQ, with 0.5 mol% NBD-PC.

and distributed uniformly over the visual fields. Such a LE to LC phase transition occurred in mixed monolayers and had features similar to those seen in pure DPPC films (see Fig. 8). The presence of 5 mol% ubiquinone decreases the LC domain size and a change in shape is observed, compared with pure DPPC at equivalent surface pressures, as shown in Fig. 8. These features are associated with an overall decrease of the total area occupied by the LC domains, as quantified in Fig. 9.

Fig. 9 shows a plot of percentages of LC domain, i.e., (total area of the condensed domains/total area of the frame)×100, versus surface pressure for DPPC containing 0 to 10 mol% ubiquinone. Each dataset presented contains the whole data of three independent experiments (i.e., three different monolayers), with images took at various surface pressures. With this procedure, standard deviations of the calculated proportions of condensed area are given by the systematic error due to preprocessing and threshold adjustment and are estimated at ±3%.

Pure DPPC monolayer begins to condense near 5 mNm^{-1} and condensed domains occupy over 60% of the total area near 6 mNm^{-1}. In monolayers containing 5–10 mol% ubiquinones, dark regions were initially observed at higher surface pressures, especially in the case of DPPC:UQ-10 mixtures; at 10 mol% condensation started at ~8 mNm^{-1}. Moreover, the images seen at 8 mNm^{-1} in Fig. 8 (B2 to B5) showed condensed domains having multilobe shapes as those observed in DPPC film compressed at the same rate to 6 mNm^{-1} (A_1).

4. Discussion

While there are several reports on UQ organization in bilayers, this is the first systematic study on the thermodynamic behavior of mixed monolayers of DPPC and ubiquinones with polyisoprenoid chain length varying from 2 to 10 isoprene units. DPPC has been selected for this investigation since a well-defined LE-LC phase transition is observed during compression. Thus, it was possible to study the influence of the UQ chain length on this DPPC phase transition by epifluorescence microscopy.

4.1. Behavior of pure UQ monolayers

As the length of the side-chain decreases, the collapse pressure of UQ monolayers decreases. To some extent, the behavior

of UQ on water surface could be interpreted as the case of fatty acids and must be related to a shift in the balance of hydrophobic to hydrophilic character of the molecule in favor of greater polarity. Indeed, this behavior can be rationalized in terms of competition of two major factors: the effect of a relatively polar headgroup and the presence of an hydrophobic isoprenoid tail. The longer the chain is, the greater the hydrophobic properties are. The cyclohexane/water partition coefficients and the retention times in HPLC analysis of different ubiquinones known from literature [49,50] are good parameters of their hydrophobicity. It was observed that each isoprene unit increases the partition coefficient by approximately 2.5 orders of magnitude and causes more pronounced changes in the retention times for long homologues in comparison to the short quinones. Thus, the lateral chain length governs directly the hydrophobic/hydrophilic balance of ubiquinones and the collapse point is a good marker of their hydrophobicity. However, after the collapse point, all UQ films remain very stable for several hours, in contrast with fatty acids [51]. This difference is probably correlative to the nature of the headgroup: the packing of benzoquinone rings can certainly stabilize the monolayers.

UQ4 and UQ6, with middle long chains, form monolayers the less sensitive to loss of material upon compression. UQ2 with the shortest hydrophobic tail (only 10 carbon atoms), and UQ10 with the longest one, are squeezed out more easily from the films during compression. Comparison with fatty acids helps to clarify the nature of material loss. Indeed, the water solubility of fatty acids decreases as the alkyl chain increases. To obtain an insoluble monolayer of a non-ionized fatty acid, the molecule must contain at least twelve carbon atoms [52]. In our cases, the shortest ubiquinone, UQ2, cannot maintain at the air/water interface due to its weak hydrophobicity and then dissolves into the water subphase. In contrast, longer derivatives must be gradually expelled above the monolayer. This is the case of the longest derivative, UQ10, which contains an isoprenoid chain that when fully extended is more than twice the length of the fatty acyl residues of a DPPC molecule and forms monolayers with the lowest collapse pressure.

In addition, the molecular area occupied by UQ at a given surface pressure increases with the side chain length. It is noteworthy that each isoprene unit contains an insaturation in position 2 and a branched methyl group in position 3. Interestingly, films of branched/unsaturated fatty acids tend to be expanded rather than condensed, compared with saturated/unbranched fatty acids [46]. Then, as in the case of unsaturated and/or branched fatty acids [52], isoprenoid chains disturb close packing in UQ monolayers, the expansion of the film depending on chain length too.

4.2. Mixed UQ:DPPC monolayers

Based on the composition-dependent collapse surface pressures, it can be concluded that DPPC and UQn were totally or partially miscible at the air/water interface except for mixtures containing more than 50 mol% UQ10. The presence of UQn in DPPC monolayers disturbs the packing of DPPC molecules in a nonideal way, and results in the formation of a biphasic system with positive deviations in A_{ex} which are more pronounced as the isoprenoid chain is longer. This behavior can be explained by the difference in the side chain lengths of both components in the mixed monolayers, side-chains of UQ6 and UQ10 being longer than the hydrocarbon chains of DPPC. Indeed, the parts of UQ6 or UQ10 molecules which protrude from the monolayer can freely rotate over phospholipid molecules and strongly interact by steric repulsions in ubiquinones-rich microdomains, due to insaturations and branched methyl groups. Thus, the space occupied by UQ6 or UQ10 chains increases the average molecular area. The highest deviation should then occurs at equal amount of DPPC and UQ molecules, which is consistent with the experimental data obtained (Fig. 6). To explain this $A_{ex}=f(X_{UQ})$ profile, we propose, as stated before, that the relative organization of the two components remains unchanged whatever their proportion. A convenient model would be that, as the long-chain ubiquinones molar fraction increases, the number of UQn-rich microdomains increases, their size remaining unchanged. Hence, with this microdomains constant size model, we can explain why the quantity of individual interactions between the two components depends only on their relative proportion. The length of the fully extended UQ4 is approximately the same as the DPPC when both the molecules are oriented vertically in the film, whereas the length of UQ2 side-chain is shorter. However, at 10 mNm^{-1}, the mean molecular area is still higher than that of ideally mixed components, indicating that UQ2 and UQ4 do no pack ideally between the hydrocarbon chains of the phospholipids, but form UQn-rich microdomains. As stated before, the asymmetry of the $A_{ex}=f(X_{UQ})$ profile in case of short-chain ubiquinones suggests that DPPC:UQn interactions in mixed films would be minimized by means of a change in the relative organization of the two components, that results in a growth of the UQn-rich microdomains size as the ubiquinone molar fraction increases. This would be possible thanks to the nature of global interactions between short-chain ubiquinones in UQn-rich microdomains, where van der Waals attractions would be able to compensate steric repulsions. It is interesting to note that at low contents of ubiquinones (i.e., $\leq$10 mol%), the presence of UQ2 perturbs more the packing of DPPC molecules than UQ4. For 25 or more mol% ubiquinones, the excess area is higher with UQ4 than UQ2. This suggests that above this content, unsaturated and non branched UQ2 chains allow more UQ chain–UQ chain van der Waals interactions than the UQ4 isoprenoid tails, within UQ-rich microdomains.

Moreover, the decrease of the excess area per molecule for surface pressures higher than 10 mNm^{-1} could be interpreted in two distinct ways: (i) as the surface pressure increases the system can tend towards a total segregation, (ii) as π becomes close to the collapse pressure, ubiquinones are gradually expelled from the monolayer. However, explanation (ii) must be excluded since gradual expulsion of UQ over compression would have implied ΔG_m decrease as well. In addition, by plotting mixed films isotherms as a function of the area per DPPC molecule (Fig. 4), it can be seen that ubiquinones seem largely excluded from monolayers only for surface pressures widely larger than the collapse pressure of the pure UQn, which is the limiting data to calculate

A_{ex} and ΔG_m. Then, these parameters may be not suitable to account for the expulsion of ubiquinones from monolayers. The hypothesis (i) is not either fully satisfactory, since the composition-dependence of collapse surface pressures noticed in the previous section (Fig. 5) does not argue for total segregation, even if the positive ΔG_{ex} values are nevertheless compatible with. Thus, the system must tend towards a more marked segregation, the microdomains being certainly more and more pure as the pressure increases. However, the total lateral segregation is never reached because film collapse occurs before it can be effective. Similar to pure ubiquinones monolayers, this film collapse could mainly result in the formation of a disordered UQn-rich phase overlying the system. With DPPC:UQ2 mixtures dissolution of the ubiquinone into the water subphase could be envisaged.

Fluorescence microscopy has been used in studying mixed monolayers. Systematically the higher the proportion of ubiquinone, the lower the percentage of LC domains are observed at higher surface pressures. Increasing amounts of ubiquinone resulted in a decreased amount of probe-excluded regions even at high surface pressures, i.e., favoring the existence of continuous bright field. Thus, ubiquinones seem to be preferentially soluble in this continuous phase. Ubiquinones disrupt DPPC packing and decrease the size of the dark ordered condensed domains while increasing that of the disordered phase. Longer is the isoprenoid chain more pronounced is the effect.

The condensed domains observed in mixed monolayers at 8 mNm^{-1} show multilobe shapes as those observed in DPPC film at 6 mNm^{-1}. This observation would tend to suggest that the condensed domains of mixed DPPC:UQ_n films may be made of the main component, the DPPC. Consequently, miscibility of DPPC and UQ could be assumed to decrease when condensed regions become majority. This is coherent with previous results showing that deviations from ideality are strongly increased in the corresponding surface pressure range.

In conclusion, when mixed with DPPC, ubiquinones exhibit distinct lateral organizations, depending also on the length of side-chain. Long-chain ubiquinones (UQ6 and UQ10) are self-organized within UQn-rich constant-size microdomains, while short-chain ubiquinones (UQ2 and UQ4) form microdomains able to grow as the ubiquinone concentration increases. Over 2D compression, the system tends to a total DPPC/UQ lateral segregation, ubiquinones being preferentially soluble in the continuous expanded phase. However, this total segregation is never reached due to transversal expulsion of film compounds, mainly ubiquinones. Similarly to pure ubiquinone films, collapse surface pressure of DPPC:UQ mixed films depends on the side-chain length too. Expulsion occurs for surface pressures as low as the lateral chain is long and may result in the formation of a disordered UQn-rich phase overlying the monolayer.

Our study gives strong evidence for an influence of isoprenoid chain length on both the lateral organization and the transversal expulsion of ubiquinones within DPPC:UQ monolayers.

4.3. Outlook

Although some concentrations used in this study are higher than in the native systems, the results can give us some information about the influence of the chain length on the orientation of ubiquinones in membranes, bearing in mind the limitations of an analogy between a monolayer model system and the biological membrane.

Thus, chain-length effects occurring in model membranes could be related with previously described differences on biological actions and therapeutic effects from short-chain exogenous derivatives compared to natural human UQ10. Our results support a preferential midplane location of UQ10 in biological membranes, whereas, in similar conditions, short-chain (UQ2, UQ4) exogenous derivatives would be able to remain oriented parallel to the chains of the phospholipids with their quinone domains in the region of the phospholipids headgroup. This conclusion is supported by many authors having studied ubiquinones localization within phospholipids bilayers by various techniques [32–36,38–41]. In addition, according to our model, it is proposed that lateral organization of UQ10 and short-chain derivatives in membranes would be different: respectively, (i) formation of an increasing number of ubiquinones-rich microdomains of a limited size, and (ii) organization of UQ analogues within less growth limited microdomains. Such a lateral organization of UQn-rich domains supports the distribution of ubiquinone in separate and distinct pools within biological membranes as previously suggested [53]. One can propose exogenous short-chain analogues to form larger pools than natural UQ10 molecules, in the same physiological conditions, that would be of great significance for some specific biological roles, especially when interactions with other functional lipids or membrane proteins are involved. This assumption is supported by some studies that have shown that mitochondrial complex I has two distinct anchoring sites for short and long chain ubiquinones [28–30]. Such functional specificity of short-chain ubiquinones could be correlated to their noteworthy therapeutic efficiency [27] and argue for isoprenoid chain length to be an essential tune able parameter for new drugs design.

References

[1] M.D. Collins, Analysis of isoprenoid quinones, in: A. Press (Ed.), Methods in Microbiology, vol. 18, Academic Press, London, 1985, pp. 329–363.
[2] G.P. Moss, IUPAC-IUB Commission on Biochemical Nomenclature, vol. 2002, 1973.
[3] F.L. Crane, Y. Hatefi, R.L. Lester, C. Widmer, Biochim. Biophys. Acta 25 (1957) 220–221.
[4] R.A. Morton, G.M. Wilson, J.S. Lowe, Leat, Biochem. J. 68 (1958).
[5] L. Ernster, G. Dallner, Biochemical, physiological and medical aspects of ubiquinone function, Biochim. Biophys. Acta 1271 (1995) 195–204.
[6] P. Mitchell, Protonmotive Q cycle. General formulation, FEBS Lett. 59 (1975) 137–139.
[7] U. Brandt, B. Trumpower, The protonmotive Q cycle in mitochondria and bacteria, Crit. Rev. Biochem. Mol. Biol. 29 (1994) 165–197.
[8] H.P. Kaufmann, H. Garloff, Pro- and antioxidants in fats. II. Naturally occurring antioxidants. 1, Fette, Seifen, Anstrichmittel 63 (1961) 334–344.
[9] V.E. Kagan, J.P. Fabisiak, P.J. Quinn, Coenzyme Q and vitamin E need each other as antioxidants, Protoplasma (2000) 11–18.
[10] H. Nohl, L. Gille, K. Staniek, The biochemical, pathophysiological, and medical aspects of ubiquinone function, Ann. N.Y. Acad. Sci. 854 (1998) 394–409.
[11] F.L. Crane, P. Navas, The diversity of coenzyme Q function, Mol. Aspects Med. 18 (1997) S1–S6.

[12] F.L. Crane, New functions for coenzyme Q, Protoplasma (2000) 127–133.
[13] C. Gomez-Diaz, M.P. Barroso, P. Navas, Plasma membrane coenzyme Q10 and growth control, Protoplasma (2000) 19–23.
[14] R. Alleva, M. Tomasetti, L. Andera, N. Gellert, B. Borghi, C. Weber, M.P. Murphy, J. Neuzil, Coenzyme Q blocks biochemical but not receptor-mediated apoptosis by increasing mitochondrial antioxidant protection, FEBS Lett. 503 (2001) 46–50.
[15] T. Kagan, C. Davis, L. Lin, Z. Zakeri, Coenzyme Q10 can in some circumstances block apoptosis, and this effect is mediated through mitochondria, Ann. N.Y. Acad. Sci. 887 (1999) 31–47.
[16] C. Sobreira, M. Hirano, S. Shanske, R.K. Keller, R.G. Haller, E. Davidson, F.M. Santorelli, A.F. Miranda, E. Bonilla, Mojon, et al., Mitochondrial encephalomyopathy with coenzyme Q10 deficiency, Neurology 48 (1997) 1238–1243.
[17] A. Rotig, E.L. Appelkvist, V. Geromel, D. Chretien, N. Kadhom, P. Edery, M. Lebideau, G. Dallner, A. Munnich, Ernster, et al., Quinone-responsive multiple respiratory-chain dysfunction due to widespread coenzyme Q10 deficiency, Lancet 356 (2000) 391–395.
[18] E. Boitier, F. Degoul, I. Desguerre, C. Charpentier, D. Francois, G. Ponsot, M. Diry, P. Rustin, C. Marsac, A case of mitochondrial encephalomyopathy associated with a muscle coenzyme Q10 deficiency, J. Neurol. Sci. 156 (1998) 41–46.
[19] Y. Ihara, R. Namba, S. Kuroda, T. Sato, T. Shirabe, Mitochondrial encephalomyopathy (MELAS): pathological study and successful therapy with coenzyme Q10 and idebenone, J. Neurol. Sci. 90 (1989) 263–271.
[20] O. Musumeci, A. Naini, A.E. Slonim, N. Skavin, G.L. Hadjigeorgiou, N. Krawiecki, B.M. Weissman, C.Y. Tsao, J.R. Mendell, Shanske, et al., Familial cerebellar ataxia with muscle coenzyme Q10 deficiency, Neurology 56 (2001) 849–855.
[21] Langsjoen, P. (1994).
[22] E.K. Ruuge, K.P. Kashkarov, V.L. Lakomkin, A.A. Timoshin, E.V. Vasil'eva, The redox state of coenzyme Q10 in mitochondrial respiratory chain and oxygen-derived free radical generation in cardiac cells, Mol. Aspects Med. 18 (1997) s41–s50.
[23] S.T. Sinatra, Refractory congestive heart failure successfully managed with high dose coenzyme Q10 administration, Mol. Aspects Med. 18 (1997) s299–s305.
[24] A.W. Linnane, M. Degli Esposti, M. Generowicz, A.R. Luff, P. Nagley, The universality of bioenergetic disease and amelioration with redox therapy, Biochim. Biophys. Acta 1271 (1995) 191–194.
[25] A.W. Linnane, S. Kovalenko, E.B. Gingold, The universality of bioenergetic disease. Age-associated cellular bioenergetic degradation and amelioration therapy, Ann. N.Y. Acad. Sci. 854 (1998) 202–213.
[26] E.B. Gingold, G. Kopsidas, A.W. Linnane, Coenzyme Q10 and its putative role in the ageing process, Protoplasma (2000) 24–32.
[27] T. Lerman-Sagie, P. Rustin, D. Lev, M. Yanoov, E. Leshinsky-Silver, A. Sagie, T. Ben-Gal, A. Munnich, Dramatic improvement in mitochondrial cardiomyopathy following treatment with idebenone, J. Inherit. Metab. Dis. 24 (2001) 28–34.
[28] L. Helfenbaum, A. Ngo, A. Ghelli, A.W. Linnane, M. Degli Esposti, Proton pumping of mitochondrial complex I: differential activation by analogs of ubiquinone, J. Bioenerg. Biomembranes 29 (1997) 71–80.
[29] M. Degli Esposti, A. Ngo, G.L. McMullen, A. Ghelli, F. Sparla, B. Benelli, M. Ratta, A.W. Linnane, The specificity of mitochondrial complex I for ubiquinones, Biochem. J. 313 (Pt 1) (1996) 327–334.
[30] H. Miyoshi, Probing the ubiquinone reduction site in bovine mitochondrial complex I using a series of synthetic ubiquinones and inhibitors, J. Bioenerg. Biomembranes 33 (2001) 223–231.
[31] S. Bernard, Y. Roche, F. Etienne, P. Peretti, Interaction between ubiquinones and dipalmitoylphosphatidylcholine in mixed Langmuir monolayers, Mol. Cryst. Liquid Cryst. Sci. Technol., Sect. A Mol. Cryst. Liquid Cryst. 338 (2000) 207–221.
[32] E.L. Ulrich, M.E. Girvin, W.A. Cramer, J.L. Markley, Biochemistry 24 (1985) 2501–2508.
[33] G. Metz, K.P. Howard, W.B.S. van Liemt, J.H. Prestegard, J. Lugtenburg, S.O. Smith, J. Am. Chem. Soc. 117 (1995) 564–565.
[34] A. Alonso, J.C. Gomez-Fernandez, F.J. Aranda, F.J.F. Belda, F.M. Goni, On the interaction of ubiquinones with phospholipid bilayers, FEBS Lett. 132 (1981) 19–22.
[35] H. Katsikas, P.J. Quinn, The polyisoprenoid chain length influences the interaction of ubiquinones with phospholipid bilayers, Biochim. Biophys. Acta (BBA), Biomembr. 689 (1982) 363–369.
[36] M. Jemiola-Rzeminska, B. Mysliwa-Kurdziel, K. Strzalka, The influence of structure and redox state of prenylquinones on thermotropic phase behaviour of phospholipids in model membranes, Chem. Phys. Lipids 114 (2002) 169–180.
[37] M. Jemiola-Rzeminska, J. Kruk, M. Skowronek, K. Strzalka, Location of ubiquinone homologues in liposome membranes studied by fluorescence anisotropy of diphenyl-hexatriene and trimethylammonium-diphenyl-hexatriene, Chem. Phys. Lipids 79 (1996) 55–63.
[38] G. Lenaz, B. Samori, R. Fato, M. Battino, G. Parenti Castelli, I. Domini, Localization and preferred orientations of ubiquinone homologs in model bilayers, Biochem. Cell. Biol. 70 (1992) 504–514.
[39] B. Samori, G. Lenaz, M. Battino, G. Marconi, I. Domini, On coenzyme Q orientation in membranes: a linear dichroism study of ubiquinones in a model bilayer, J. Membr. Biol. 128 (1992) 193–203.
[40] T. Hauss, S. Dante, T.H. Haines, N.A. Dencher, Localization of coenzyme Q10 in the center of a deuterated lipid membrane by neutron diffraction, Biochim. Biophys. Acta (BBA), Bioenerg. 1710 (2005) 57–62.
[41] T. Hauss, S. Dante, N.A. Dencher, T.H. Haines, Squalane is in the midplane of the lipid bilayer: implications for its function as a proton permeability barrier, Biochim. Biophys. Acta (BBA), Bioenerg. 1556 (2002) 149–154.
[42] P.J. Quinn, M.A. Esfahani, Ubiquinones have surface-active properties suited to transport electrons and protons across membranes, Biochem. J. 185 (1980) 715–722.
[43] S. Sharma, T.P. Radhakrishnan, Phospholipid-fatty acid composite monolayers: analysis of the pressure-area isotherms, Thin Solid Films 382 (2001) 246–256.
[44] S. Wu, Intermolecular interaction in some mixed polymer monolayers at the air–water interface, J. Colloid Interface Sci. 29 (1969) 139–147.
[45] P. Dynarowicz-Latka, K. Kita, Molecular interaction in mixed monolayers at the air/water interface, Adv. Colloid Interface Sci. 79 (1999) 1–17.
[46] G.L.J. Gaines, in: I. Prigogine (Ed.), Interscience Monographs on Physical Chemistry, John Wiley and Son Inc, 1966.
[47] M.N. Jones, D. Chapman, Micelles, Monolayers and Biomembranes, Wiley-Liss, Inc., 1995.
[48] F.C. Goodrich, International Congress of Surface Activity, 1957, p. 8591.
[49] G. Lenaz, Quinone specificity of Complex I, Biochim. Biophys. Acta (BBA), Bioenerg. 1364 (1998) 207–221.
[50] M. Jemiota-Rzeminska, D. Latowski, K. Strzalka, Incorporation of plastoquinone and ubiquinone into liposome membranes studied by HPLC analysis. The effect of side chain length and redox state of quinone, Chem. Phys. Lipids 110 (2001) 85–94.
[51] R. Heikkila, C. Kwong, D. Cornwell, Stability of fatty acid monolayers and the relationship between equilibrium spreading pressure, phase transformation, and polymorphic crystal form, J. Lipid Res. 11 (1970) 190–194.
[52] M.C. Petty, Langmuir-Blodgett Films, an Introduction, Cambridge University Press, 1996.
[53] G. Lenaz, A critical appraisal of the mitochondrial coenzyme Q pool, FEBS Lett. 509 (2001) 151–155.